

Behavior of reinforcing bar connections of hollow-core slabs to masonry walls under in-plane forces

Susana Hernandez Brito, Karam Mahmoud, Karl Truderung, and Ehab El-Salakawy

- Nine full-scale assemblies of hollow-core slab reinforcing bar connections to masonry beams were tested under in-plane monotonic forces until failure.
- The variables of the test specimens included bearing type (end-bearing or side-bearing connection), load direction (compression or tension against the masonry beam), and load orientation (normal or parallel to the longitudinal axis of the masonry beam). In addition, the effect of using an adhesive to enhance bar bonding to the masonry beam was examined in two of the end-bearing connections.
- The failure mode for each specimen was examined in the test program.

Hollow-core slabs are commonly selected to span large areas in residential and industrial buildings where clear and open spaces are required. In 2016, it was estimated that more than 50 million m² (538 million ft²) of hollow-core slab floors have been constructed in Canada since 1962.¹ These slabs have relatively lightweight and shallow cross sections compared with other precast, prestressed solid concrete slabs with similar load-carrying capacities. The voids in hollow-core slabs eliminate up to 50% of the concrete volume in the geometric center of the section, where the slabs do not carry flexure, allowing longer spans, reduced deflections, and smaller section heights.

Hollow-core slab floors are typically designed to act as continuous horizontal diaphragms, where lateral in-plane loads (such as winds, earthquakes, or accidental loads during construction) are transferred to lateral force-resisting walls throughout their bearing connections. There are two types of connections:

- end-bearing connection: hollow-core slab transfers the gravity loads onto the supporting element at the bearing ends
- side-bearing connection: the hollow-core slab transfers the loads onto the supporting element on its longitudinal edge

Depending on their direction, lateral in-plane loads result in axial or shear forces in hollow-core slab bearing connections.

Besides horizontal load transfer to supporting members, the use of steel reinforcement in bearing connections is intended for structural integrity and to prevent slab displacements that could result in floor misalignments, loss of bearing, or even a progressive collapse. Furthermore, the connection reinforcement provides lateral bracing for the axially loaded supporting members by connecting bearing walls to the floor diaphragm.

Due to the main function of this connection reinforcement, current North American design codes CSA Group (CSA) A23.3-19² and American Concrete Institute's *Building Code Requirements for Structural Concrete (ACI 318-19) and Commentary (ACI 318R-19)*³ refer to them as integrity ties, in which the tie resistance shall be governed by yielding of the steel component, assumed to be a reinforcing bar for hollow-core slab connections. Accordingly, these codes require minimum threshold design loads to achieve structural integrity via tension ties that connect the hollow-core slab diaphragms to the end walls of the building. For structures up to two stories high, CSA A23.3-19 requires that connections between the hollow-core slab diaphragm and laterally supported elements be designed for a minimum factored tensile resistance of not less than 5.0 kN/m (0.34 kip/ft), with ACI 318-19 requiring a slightly lower minimum force of 4.4 kN/m (0.30 kip/ft). However, for structures that are three or more stories high and are constructed with precast concrete bearing walls, CSA A23.3-19 and ACI 318-19 require a minimum factored tensile resistance of 14 or 22 kN/m (0.96 or 1.51 kip/ft) of supporting wall length, respectively, for longitudinal tension ties in end-bearing connections.

A possible reason for the lower CSA A23.3-19² design tensile resistance value of 14 kN/m (0.96 kip/ft) compared with the ACI 318-19³ design value of 22 kN/m (1.51 kip/ft) could be that a 10M (no. 3) reinforcing bar placed at every second hollow-core slab joint at a spacing of 2440 mm (96 in.) would require a minimum factored resistance of 34 kN (7.64 kip) per bar, which is exactly the factored resistance of a single 10M bar in tension. For hybrid structures, such as a multilevel building constructed with masonry walls and hollow-core slabs, no specific design provisions apply; however, it would be logical that the minimum recommended tension tie force thresholds given in CSA A23.3-19 and ACI 318-19 could be reasonably applied based on the number of stories in the building.

For design calculations, the tie spacing selected depends on the individual capacity of each tie. Although these code minimum force requirements are intended only for integrity ties under tension or pulling forces, compression and shear forces act equally on hollow-core slab floors due to the reversible nature of lateral loads (for example, wind loads, seismic loads, and accidental loads). Therefore, hollow-core slab connections must be able to resist compression, tension, or shear forces to provide a complete load path between critical elements throughout the building under response from lateral loads and still maintain a minimum level of structural integrity.

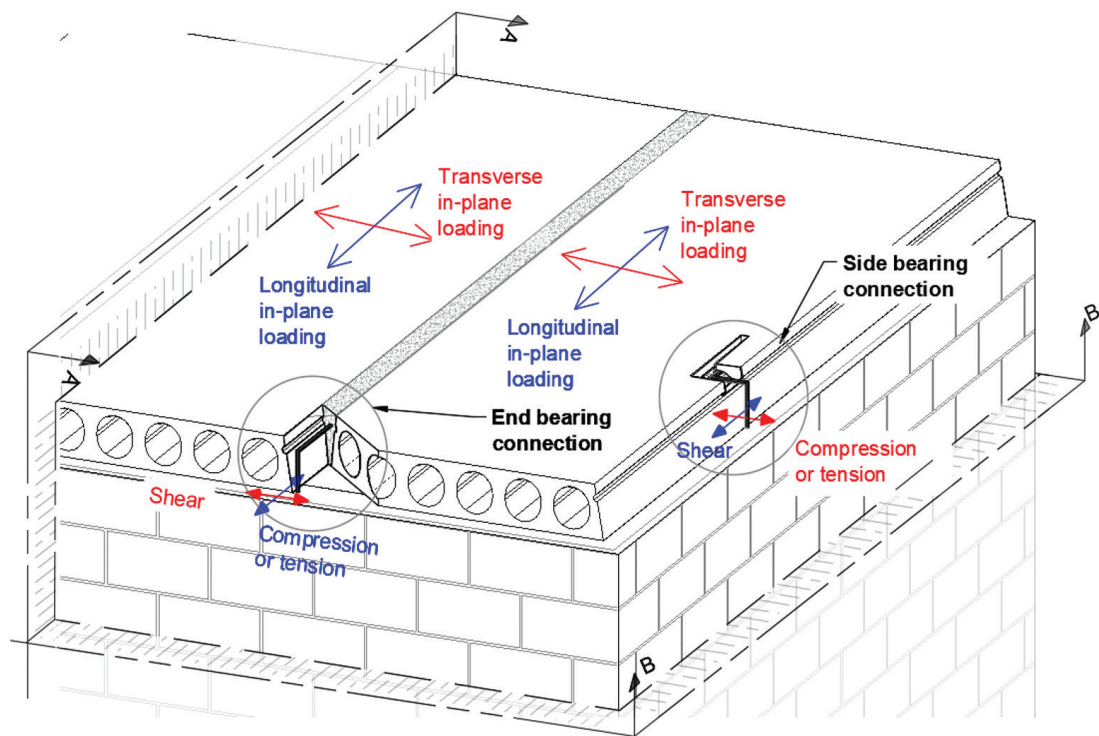
Background and motivation

In Eastern Canada, an integrity tie typically consists of an L-shaped, 10M (no. 3) Grade 400W (58 ksi) steel reinforcing bar (**Fig. 1**). This connection bar is hammered 150 mm (5.9 in.) into the masonry wall from one end and grouted to the shear keys or side cores of the hollow-core slab on the other end. A tight hole is drilled on top of the masonry wall, required to achieve a strong fixation of the embedded portion of the vertical leg of the bar, via direct bar contact with the masonry grout and without using a binding material such as epoxy. In end-bearing connections, one connection bar is inserted between hollow-core slabs (spacing of 1220 mm [48 in.]), while in side-bearing connections, bars are inserted into side pockets (maximum spacing of 3000 mm [118 in.]). These pockets are saw-cut slots that are preordered from the manufacturer of the slabs. It is a common practice to provide a minimum embedment length in grout of at least 450 mm (17.7 in.) to ensure a strong anchorage of the reinforcing bar to the hollow-core slab.

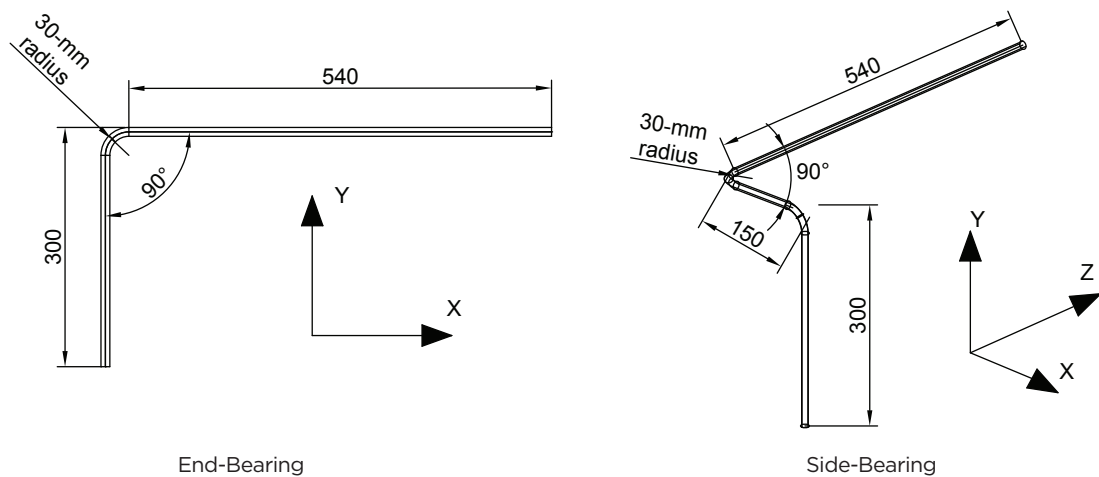
Another typical bearing connection detail consists of grouting one end of the L-shaped bar to the shear keys or side pockets of the hollow-core slab while leaving its other end exposed and facing upward to be inserted into the next masonry course constructed above the hollow-core slab.^{4,5} That course of masonry blocks is then filled with grout around the connection bar. As an alternative to L-shaped ties, U-shaped hooked bars can also be employed to connect hollow-core slabs to supporting masonry walls. In this case, the steel hooks are tied to the longitudinal steel reinforcement of boundary elements cast at the top of the masonry wall and cast integrally. Afterward, the other ends of the hooks are grouted to the shear keys or pockets of the hollow-core slabs.

Despite the wide use of reinforcing bar connections in Eastern Canada, current design codes and guidelines do not offer a design methodology or sufficient provisions for their design and construction.²⁻⁵ These standards suggest using the shear friction theory to determine the horizontal-load capacity of hollow-core slab bearing connections. However, due to the eccentricity between the entry and exit points of lateral loads in the overall connection system (from the hollow-core slab grout key into the masonry wall at the base of the slab below), shear friction may not be appropriate for analysis of such connections (**Fig. 2**). In addition, there has been no research on the behavior of hollow-core slab bearing connections to masonry wall supports. Previous studies covered the seismic performance of hollow-core slab diaphragms supported on concrete beams, where the bearing connections were cast integrally and behaved compositely.⁶⁻¹⁰

To the authors' knowledge, no research has been conducted on the lateral resistance of hollow-core slab bearing connections to masonry walls using the detailing commonly used in Eastern Canada for integrity ties. Therefore, it is deemed necessary to investigate the capacity and the mode of failure of the reinforcing bar connection under in-plane forces.



End- and Side-bearing connections of HCS supported on masonry walls



End-Bearing

Side-Bearing

Figure 1. Connection bar details. Note: Dimensions are in millimeters. 1 mm = 0.0394 in.

Experimental program

Test specimens

Nine full-scale assemblies of hollow-core slab reinforcing bar connections to masonry beams were tested under in-plane monotonic forces until failure. The assemblies were divided into two testing series according to the bearing type (**Table 1**), where series I corresponded to end-bearing connections (five specimens) and series II was dedicated to side-bearing connections (four specimens). The specimens were constructed

with 203 mm (8 in.) thick hollow-core slabs cut into 1220 mm (48 in.) square segments. For end-bearing connections, two of these segments were employed to assemble the connection, whereas side-bearing connections involved a single segment of hollow-core slab. The slabs were supported on a two-course, 190 mm (7.5 in.) wide single wythe masonry beam of 3200 mm (126 in.) length, which simulated the typical bond beam constructed with U masonry blocks at the top of the wall. The longitudinal reinforcement of the masonry beam consisted of two 10M (no. 3) steel bars placed inside the U blocks, which were filled with grout. The masonry beam was made of 190 ×

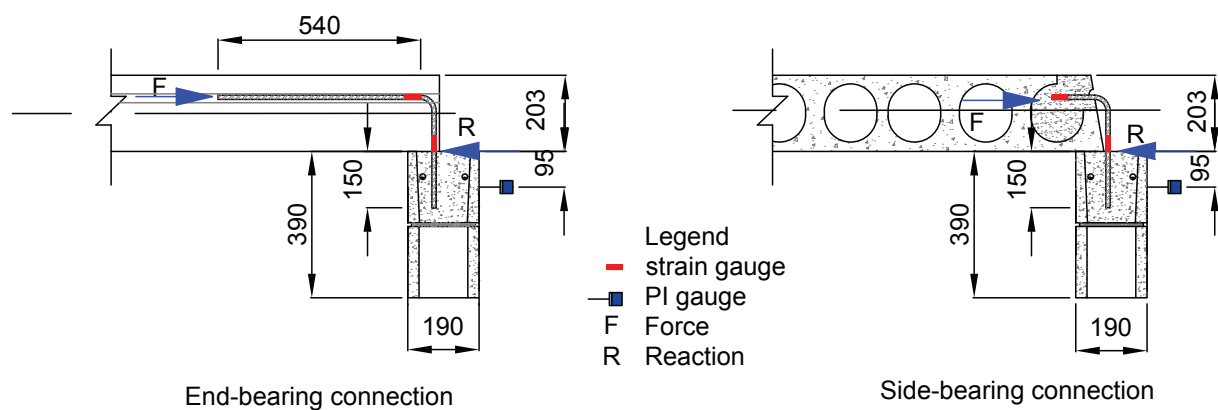


Figure 2. Steel bar connection detailing, locations of gauges, and force eccentricity. Note: Dimensions are in millimeters. 1 mm = 0.0394 in.

Table 1. Details of test specimens

Specimen code	Series	Type of connection	Load direction	Load orientation	Bar installation
EB-CN-A	I	End-bearing connection	Compression	Normal to support axis	Adhesive
EB-CN-D	I	End-bearing connection	Compression	Normal to support axis	Dry fit
EB-TN-A	I	End-bearing connection	Tension	Normal to support axis	Adhesive
EB-TN-D	I	End-bearing connection	Tension	Normal to support axis	Dry fit
EB-CP-D	I	End-bearing connection	Compression	Parallel to support axis	Dry fit
SB-CN-D	II	Side-bearing connection	Compression	Normal to support axis	Dry fit
SB-TN-D	II	Side-bearing connection	Tension	Normal to support axis	Dry fit
SB-CP-D	II	Side-bearing connection	Compression	Parallel to support axis	Dry fit
SB-TP-D	II	Side-bearing connection	Tension	Parallel to support axis	Dry fit

190 × 390 mm (7.5 × 7.5 × 15.4 in.) masonry blocks in three shapes: plain end units, two-cell stretchers, and knockout web bond blocks. The masonry beams were constructed by certified masons to reproduce a high-quality construction practice.

The hollow-core slabs in both series were connected to the masonry beam using an L-shaped 10M (no. 3) connection bar or integrity tie (Fig. 1 and 2). After drilling the beam with an appropriate diameter (10 mm) bit, the hole was blown with compressed air and thoroughly vacuumed. Next, the bar was hammered into the masonry beam. An epoxy resin adhesive was incorporated into two of the end-bearing specimens to bond the bar to the masonry beam. In specimens with epoxy adhesive, the bar was hammered into the hole after injecting the adhesive using a specialized gun as specified by the supplier. Once the connection bar was installed on the masonry beam, the slabs were erected while providing a minimum seating (bearing) length of 75 mm (3 in.), which is the industry standard in North America. This value of seating length exceeded the minimum required length of 50 mm (2 in.)

according to Canadian Standards^{2,4} to prolong the test and ensure failure while the slabs are still supported. Slab spacing was set to fit the connection bar tightly, as done in practice. Finally, the connections were grouted. The hollow-core slab segments were provided by a local Canadian Precast Concrete Quality Assurance–certified precast concrete manufacturer, and the components were constructed and assembled at the Heavy Structures Laboratory of the University of Manitoba.

The test variables in this study were bearing type (end-bearing or side-bearing connection), load direction (pulling or pushing against the masonry beam), and load orientation (normal or parallel to the longitudinal axis of the masonry beam). These test variables were individually implemented to address all possible scenarios of axial and shear in-plane forces acting in hollow-core slab bearing connections to masonry walls. In addition, the effect of using an adhesive to enhance bar bonding to the masonry beam was examined in two of the end-bearing connections.

The specimen nomenclature contains three parts. The first part represents the bearing type of the hollow-core slab: EB for end-bearing and SB for side-bearing connections. The second part has two letters representing the load direction and load orientation: C for compression or pushing and T for tension or pulling and N for applied normal or P for parallel to the masonry beam, respectively. Finally, the last part of the specimen nomenclature refers to the method of installing the bar in the masonry beam: D for dry-fit bars and A for connection bars bonded with adhesive. Table 1 summarizes the specimen nomenclature and test variables.

Materials

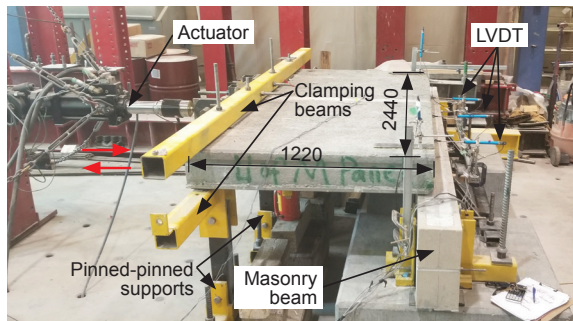
Standard tests were conducted on steel bars used for the study to determine their mechanical tensile properties, in accordance with ASTM A370-20.¹¹ The steel bars had a yielding strength, yielding strain, and modulus of elasticity of 470 ± 8 MPa (68 ± 1 ksi), $2370 \pm 40 \mu\epsilon$, and 199 GPa (28,800 ksi), respectively. Due to the lack of provisions for the construction of bearing connections in North American standards, industry-standard normal-strength grout (20 to 25 MPa [2.9 to 3.6 ksi]) was used. To obtain the grout strength on the day of testing, 51 mm (2 in.) grout cubes were cast and tested per ASTM C109/C109M-20.¹² The average grout strength obtained was 25.3 ± 3.1 MPa (3.7 ± 0.45 ksi). The

mixing, placement, and curing of this normal-strength grout were carried out according to the manufacturer's guidelines. The masonry beam was filled with a similar normal-strength grout provided by a local supplier. Finally, the hollow-core slabs were cast at the supplier's plant using concrete with a target 28-day design compressive strength of 55 to 60 MPa (8 to 8.7 ksi).

Test setup and instrumentation

The test setup contained four main components: pinned-pinned supports to allow for lateral displacement while carrying half the self-weight of the hollow-core slabs, clamping beams to distribute the in-plane forces from the actuator along the edge of the slabs, a 3200 mm (126 in.) long masonry beam, and two vertical restraints to brace the masonry beam and avoid undesired torsion at the top course of the blocks (Fig. 3). The masonry beam was fixed to the laboratory's strong floor using four steel fixtures and bars prestressed to the floor. Two rollers were attached to the masonry beam to guide the slabs and avoid slab rotation.

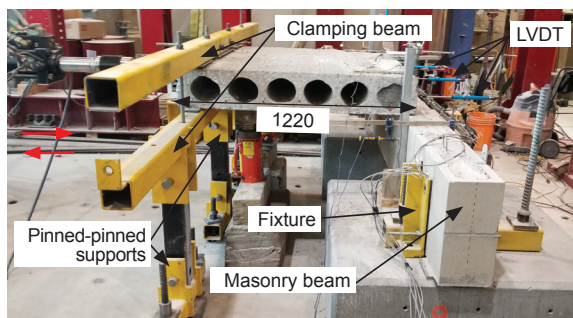
The slabs were either pulled or pushed in a parallel or normal orientation to the axis of the masonry beam. Therefore, under normal forces the connection bar resisted axial compression or tension, depending on the loading direction, and was subject-



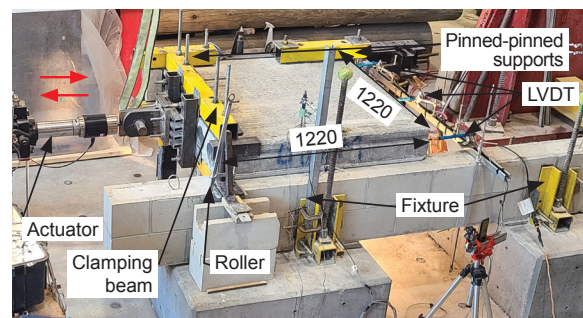
Normal load on end-bearing specimen



Parallel load on end-bearing specimen



Normal load on side-bearing specimen



Parallel load on end-bearing specimen

Figure 3. Test setup and external instrumentation. Note: Dimensions are in millimeters. 1 mm = 0.0394 in. LVDT = linear variable displacement transducer.

ed to shear under parallel forces. The loading scheme did not include additional gravity loads, other than the self-weight of the slabs, to simulate the lower-bound loading scenario with minimum friction between the slabs and the masonry beam.

An actuator with load and stroke capacities of 500 kN (112.4 kip) and ± 130 mm (± 5 in.), respectively, was mounted on a strong triangular reaction frame and hinged to the test setup. The monotonic load was applied at a rate of 5.0 mm/min (0.2 in./min) to allow gradual load application and to complete the test within 25 to 30 minutes, given the expected nominal connection capacity of 40 kN (9 kip), in direct tensile yielding of the reinforcing bar. Similar testing conditions were previously employed by Herlihy.⁶

Slab displacement was measured by linear variable displacement transducers (Fig. 3). Electrical strain gauges were used to measure strains in the connection bar close to the bends and at the beam top surface. The crack width was monitored with pi

gauges (Fig. 2), and a load cell connected to the actuator was used to record the load. Readings from these sensors were processed through a data-acquisition system. In addition, cracks, or spalling, if any, were carefully marked and photographed during the test.

Test results and discussion

The following sections discuss the test results in terms of mode of failure, capacity, measured strains in the connection bar, cracking loads, slab displacements, and overall integrity. **Table 2** summarizes the test results.

Mode of failure and cracking patterns

Series I: Loading normal to the axis of the masonry beam The mechanism of failure of end-bearing specimens subjected to normal forces depended on the loading direction: pushing or pulling. Under compression forces (pushing), the

Table 2. Test results

Type of connection	Specimen code	Mode of failure	Cracking load, kN	Yielding load, kN	Peak load, kN	Strain at peak load, $\mu\epsilon$	Slab displacement, mm*
Series I: end-bearing connection	EB-CN-A	Bar yielding and beam crushing	11.4	27.3 [†]	29.0	650	8.7
	EB-CN-D	Bar pullout, yielding, and beam fracture	4.5	20.1	25.1	16,000	84.4
	EB-TN-A	Bar cover spalling and loss of bearing	7.5	10.6	10.6	2100	36.4 [‡]
	EB-TN-D	Bar cover spalling, bar pullout, and loss of bearing	5.9	n.d.	9.2	325	5.4
	EB-CP-D	Bar yielding and pullout	13.8	18.1	25.9	10,870 [§]	112.0
Series II: side-bearing connection	SB-CN-D	Bar pullout, yielding, and beam crushing	8.2	18.2	21.2	18,650	83.1
	SB-TN-D	Bar pullout and loss of bearing	5.0	n.d.	9.1	110	60.8
	SB-CP-D	Bar yielding and pullout	n.d.	12.1	17	15,960	82.5
	SB-TP-D	Bar yielding and pullout	n.d.	7.2	7.8	4910	17.6

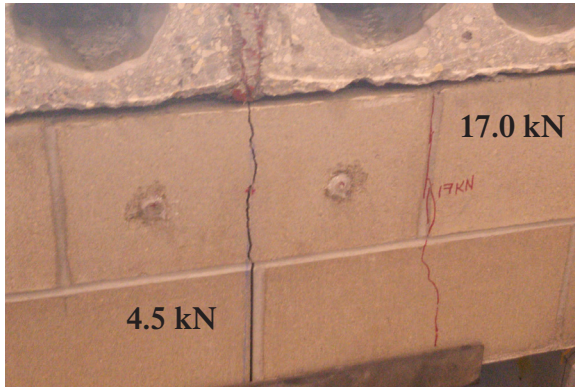
Note: EB-CN-A = end-bearing specimen with compression load applied normal to the masonry beam and connection bars bonded with adhesive; EB-CN-D = end-bearing specimen with compression load applied normal to the masonry beam and dry-fit connection bars; EB-CP-D = end-bearing specimen with compression load applied parallel to the masonry beam and dry-fit connection bars; EB-TN-A = end-bearing specimen with tension load applied normal to the masonry beam and connection bars bonded with adhesive; EB-TN-D = end-bearing specimen with tension load applied normal to the masonry beam and dry-fit connection bars; n.d. = no data; SB-CN-D = side-bearing specimen with compression load applied normal to the masonry beam and dry-fit connection bars; SB-CP-D = side-bearing specimen with compression load applied parallel to the masonry beam and dry-fit connection bars; SB-TN-D = side-bearing specimen with tension load applied normal to the masonry beam and dry-fit connection bar; SB-TP-D = side-bearing specimen with tension load applied parallel to the masonry beam and dry-fit connection bars. 1 mm = 0.0394 in.; 1 kN = 0.225 kip.

*Slab displacement at peak load.

[†]Post-peak value.

[‡]Value measured in the second peak.

[§]Measured at a load of 17.1 kN less than the peak load.



Masonry beam cracking (EB-CN-D)



Bar yielding and pull-out (EB-CN-D)



Masonry beam cracking and spalling (EB-CN-A)



Bar yielding (EB-CN-A)



Masonry beam cracking and cover spalling (EB-TN-D)



Bar deformation and pull-out (EB-TN-D)



Masonry beam cracking and spalling (EB-TN-A)



Bar yielding (EB-TN-A)

Figure 4. Mode of failure for end-bearing specimens under normal forces. Note: EB-CN-A = end-bearing specimen with compression load applied normal to the masonry beam and connection bars bonded with adhesive; EB-CN-D = end-bearing specimen with compression load applied normal to the masonry beam and dry-fit connection bars; EB-TN-A = end-bearing specimen with tension load applied normal to the masonry beam and connection bars bonded with adhesive; EB-TN-D = end-bearing specimen with tension load applied normal to the masonry beam and dry-fit connection bars. 1 mm = 0.0394 in.; 1 kN = 0.225 kip.

end-bearing connection with dry-fit bars (EB-CN-D) failed by bar pullout and yielding followed by masonry beam crushing.

Initially, at a load of 4.5 kN (1 kip), the masonry beam experienced vertical cracking in the tension side of the central masonry block at the location of the connection bar (Fig. 4). A second crack appeared at a load of approximately 17.0 kN (3.8 kip) at the vertical (head) mortar joints of the central masonry block. While the cracks propagated and widened, the connection bar experienced gradual pullout and bending in the direction of the force because, at this point, the bar lost the tight fit with the development of cracks. Figure 4 depicts the final shape of the connection bar, where the straight side inserted in the masonry beam deformed into a 90-degree bend. The cracks then propagated and connected to form a V shape, provoking spalling where the load dropped, yet the connection bar reached yielding and beam crushing ultimately occurred at a load of 25.3 kN (5.7 kip).

The mode of failure of the specimen with adhesive tested under compression (EB-CN-A) was governed by spalling of the masonry block side face followed by bar yielding and strength degradation. Like its counterpart with dry-fit bar, the vertical crack at the central block behind the bar and at the mortar head joints occurred at loads of approximately 11.4 and 25 kN (2.6 and 5.6 kip), respectively (Fig. 4). Once the spalling of the side surface of the masonry block initiated, a small load drop of 1.7 kN (0.4 kip) was observed. The bar then yielded and the load stabilized. Afterward, strength degradation occurred associated with more severe spalling, which ended with beam crushing. No bar pullout was observed during the test for the compression specimen with the adhesive.

In contrast, specimens EB-TN-D and EB-TN-A tested under tension forces failed due to loss of bearing of the slabs preceded by masonry beam spalling. The cracking patterns observed on the tension face of the masonry beam were similar to those of their counterparts tested under compression forces; however, initial vertical cracks formed at loads of 5.9 and 7.5 kN (1.3 and 1.7 kip) at the central blocks in specimens EB-TN-D and EB-TN-A, respectively (Fig. 4). These vertical cracks connected to the cracks formed at the head joint (mortar locations, at loads of 8.2 and 9.0 kN [1.8 and 2 kip]) in specimens EB-TN-D and EB-TN-A, respectively, and spalled the bar cover in both specimens.

While the specimen with dry-fit bar experienced bar pullout and strength degradation following the cover spalling, the connection bar with adhesive (EB-TN-A) reached close-to-yielding strains and a second peak of 10.6 kN (2.4 kip). Similar to their counterparts tested under compression forces, the masonry beam in the specimen with the adhesive under tension (EB-TN-A) showed more damage than its counterpart with the dry-fit bar (EB-TN-D) before the loss of bearing of the slabs. This indicates that the bar with adhesive had a better load transfer mechanism regardless of load direction.

Series I: Loading parallel to the axis of the masonry beam Under parallel pushing forces, the mode of failure of the end-bearing specimen (EB-CP-D) was characterized by bar yielding and bar pullout. Hairline cracks formed at the central block of the masonry beam and at the head joints at loads of 13.8 and 15.3 kN (3.1 and 3.4 kip), respectively (Fig. 5). However, these cracks did not propagate further or connect. Afterwards, the bar yielded while experiencing gradual pullout. Figure 5 illustrates the shape of the connec-



Masonry beam cracking (EB-CP-D)



Bar yielding (EB-CP-D)

Figure 5. Mode of failure for specimen under parallel forces. Note: EB-CP-D = end-bearing specimen with compression load applied parallel to the masonry beam and dry-fit connection bars. 1 mm = 0.0394 in.; 1 kN = 0.225 kip.

tion bar, which adopted a 90-degree bend shape, similar to the connection bar in specimen EB-CN-D tested under normal pushing (compression) force (Fig. 4).

In general, for series I, although specimens with dry-fit bars (EB-CN-D, EB-CP-D, and EB-TN-D) experienced bar pull-out, the connection bar did not detach completely from the beam. As the bar deformed, gradually yielded, and pulled out in the direction of the load, the portion that was still inside the hole acted as a lock-key mechanism, resisting the load. The longitudinal steel reinforcement in the top course of the masonry beam contributed to this lock-key mechanism by

enclosing the bar and tightening or controlling the cracks until more severe spalling occurred.

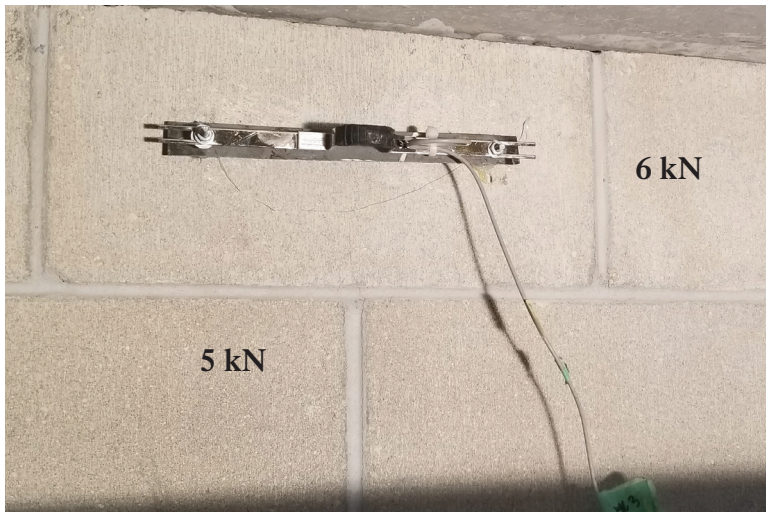
Series II: Loading normal to the axis of the masonry beam The mode of failure of the side-bearing connections had great similarity to that of their end-bearing counterparts, regardless of the load direction. Under compression forces, the side-bearing connection (SB-CN-D) failed due to bar pullout and yielding followed by masonry beam crushing. Initially, cracks formed in the masonry beam at loads of 8.2 and 17.9 kN (1.8 and 4 kip) in its center and mortar head joints, respectively (Fig. 6). With the increasing load, these cracks



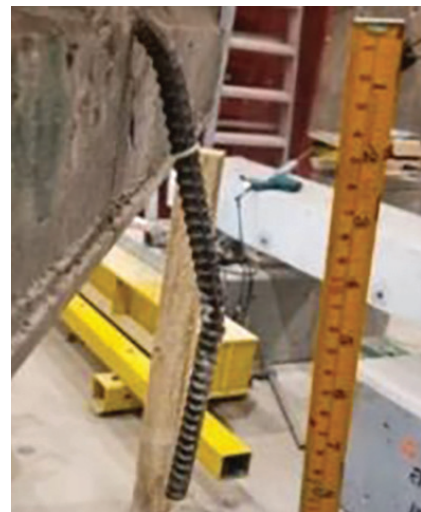
Masonry beam cracking (SB-CN-D)



Bar yielding (SB-CN-D)



Masonry beam cracking (SB-TN-D)



Bar deformation (SB-TN-D)

Figure 6. Mode of failure for side-bearing specimens under normal forces. Note: SB-CN-D = side-bearing specimen with compression load applied normal to the masonry beam and dry-fit connection bars; SB-TN-D = side-bearing specimen with tension load applied normal to the masonry beam and dry-fit connection bars. 1 mm = 0.0394 in.; 1 kN = 0.225 kip.

continued to propagate and connected to each other while the bar underwent pullout and yielded. Ultimately, the masonry beam crushed.

Under tension (pulling), the side-bearing connection (SB-TN-D) also failed because of bar pullout and loss of bearing without reaching yielding. The bar pullout was preceded by the formation of cracks at loads of 5.0 and 6.0 kN (1.1 and 1.3 kip) at the center block and masonry head joints, respectively (Fig. 6). Nevertheless, the cracks did not connect to each other before the loss of bearing of the slab, which evidenced a weaker load transfer mechanism to the masonry beam compared with its counterpart with end-bearing type.

Series II: Loading parallel to the axis of the masonry beam The mode of failure of side-bearing connections was governed by bar yielding and pullout regardless of the loading direction. No cracks formed in the masonry beam or

the hollow-core slabs while testing these specimens, which demonstrates a weak load transfer mechanism to the masonry beam. The two pictures shown in Fig. 7, corresponding to the side-bearing connections under pushing (SB-CP-D) and pulling (SB-TP-D), indicated that both connection bars had almost identical shapes at the end of testing as a result of bending in the direction of the force. In these specimens, the connection bars formed a 45-degree bend shape in the direction of the force, which significantly differed from their end-bearing counterparts.

Connection load capacity

In this study, a Grade 400W (58 ksi), 10M (no. 3) steel L-shaped bar was used to connect the hollow-core slab to the masonry beam. For a bar area of 100 mm² (0.16 in.²) and a nominal yield strength of 400 MPa (58 ksi), the expected nominal load capacity per bar location is 40 kN (9 kip),



Bar yielding (SB-CP-D)



Bar yielding (SB-TP-D)

Figure 7. Mode of failure for side-bearing specimens under parallel forces. Note: SB-CP-D = side-bearing specimen with compression load applied parallel to the masonry beam and dry-fit connection bars; SB-TP-D = side-bearing specimen with tension load applied parallel to the masonry beam and dry-fit connection bars. 1 mm = 0.0394 in.

without the application of the 0.85 material resistance factor for steel bar. For end-bearing connections, a common industry practice is to place one 10M connection bar at every grout key joint location, resulting in a bar spacing of 1220 mm (4.7 in.) for standard-width hollow-core slab.

For structures up to two stories, applying the CSA A23.3² code minimum structural integrity tension tie load of 5.0 kN/m (0.34 kip/ft) to the 10M (no. 3) L-bar connections spaced at 1220 mm (4.7 in.) requires a minimum tensile capacity of 6.1 kN (1.4 kip) per connection bar. For structures of three stories or more with precast concrete bearing walls, applying the code requirements results in minimum tensile strengths of 6.1 and 17.1 kN (1.4 and 3.8 kip) for buildings with up to two stories and with three stories or taller, respectively. If the 10M L bars can develop the full yield capacity of the reinforcing bar in tension (40 kN [9 kip]), then the nominal capacity of the bars would be more than twice the required tensile capacity for three-story buildings. Also, the minimum structural integrity force of 17.1 kN per bar would remain in the elastic range at just below 50% of the nominal yield capacity for a 10M bar.

However, the code limits^{2,3} only refer to the minimum required load capacity of structural integrity ties under tension. The designer must still verify the diaphragm tension loads resulting from the lateral load analysis and compare these tension forces with the code-specified minimum structural integrity forces. Because diaphragm lateral loads are reversible, in-plane compression and transverse (shear) forces could also be applied to the hollow-core slab floors. If these forces are not adequately addressed, the structural integrity of the floor could be compromised.

Figure 8 illustrates the recorded capacity of all specimens.

This figure also depicts code limits from ACI 318-19³ and CSA A23.3-19² as the threshold of expected capacity for all specimens based on a bar spacing of 1220 mm (4.7 in.).

Series I: Loading normal to the axis of the masonry beam The behavior of end-bearing connections tested under normal forces resulted in significant differences in the maximum load capacity depending on the loading direction. Although connections tested under compression forces (pushing) showed a more desirable mode of failure, featuring bar yielding and masonry beam crushing, the failure of specimens under tension (pulling) was governed by cover spalling and loss of bearing (seating). Therefore, the capacities of the specimens tested under compression were considerably larger than those of their counterparts under tension. When tested under compression forces, the maximum load attained was 29.0 kN (6.5 kip) at a displacement of 8.7 mm (0.34 in.) for specimen EB-CN-A and 25.1 kN (5.6 kip) at a displacement of 84.4 mm (3.3 in.) for specimen EB-CN-D. Despite the use of adhesive, which resulted in a 15.5% increase in the maximum load, the connection did not achieve the nominal yield capacity of 40 kN (9 kip) for a 10M (no. 3) bar in compression.

In contrast, end-bearing specimens tested under tension had significantly less capacity compared with their counterparts under compression. Specimen EB-TN-A reached a maximum load of 10.6 kN (2.4 kip) at a displacement of 36.4 mm (1.4 in.) in the second peak, and specimen EB-TN-D reached a maximum load of 9.2 kN (2.1 kip) at a displacement of 5.4 mm (0.2 in.). Both values were below the minimum threshold tension force of 17.1 kN (3.8 kip) recommended in CSA A23.3² for buildings of three or more stories but were still above the minimum threshold force of 6.1 kN (1.4 kip) for a structure with two stories or less. In addition, the use of adhesive resulted in a 15.2% load increase in the connection

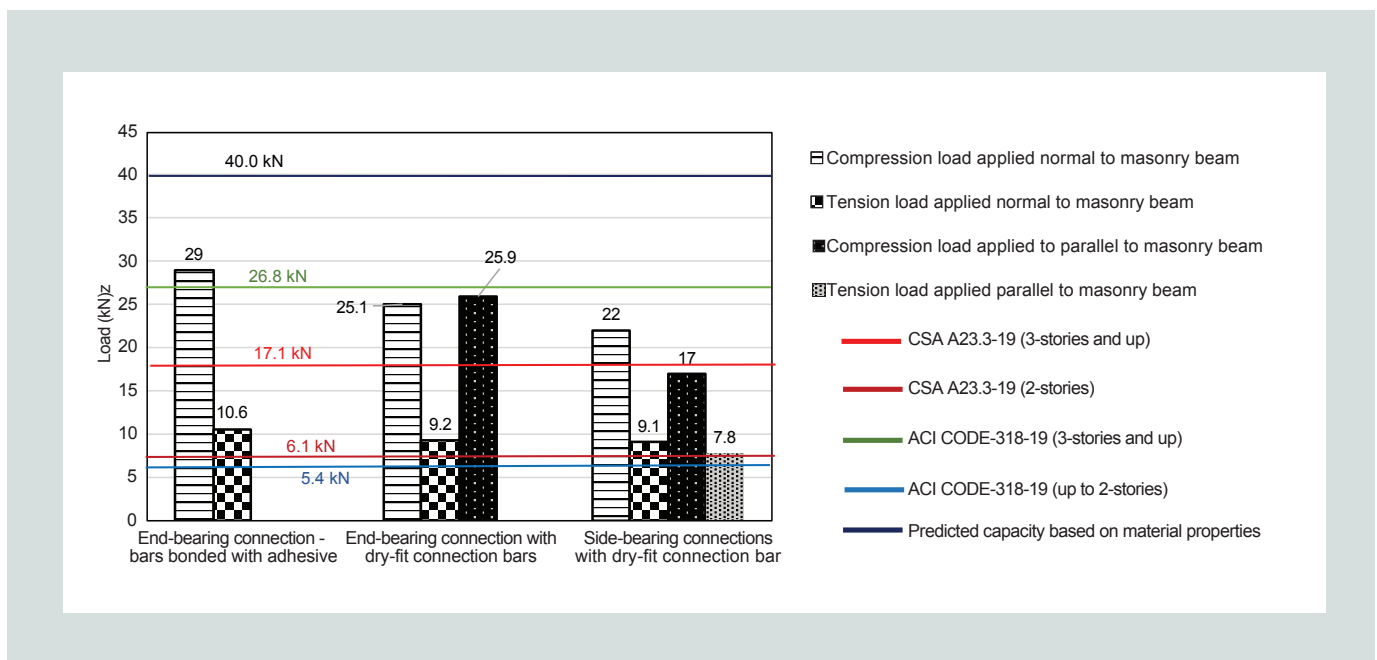


Figure 8. Connection capacity of test specimens. Note: ACI = American Concrete Institute; CSA = CSA Group. 1 kN = 0.225 kip.

capacity compared with the specimen with dry-fit bars.

Series II: Loading normal to the axis of the masonry beam The capacity of side-bearing specimens under normal forces was affected by the loading direction. The peak load in direct compression was 2.46 times higher than the tested capacity in direct tension. Whereas specimen SB-CN-D, subjected to a pushing force, failed at a peak load of 22 kN (4.9 kip) at a displacement of 83.1 mm (3.3 in.), specimen SB-TN-D, under pulling force, achieved a peak load capacity of only 9.1 kN (2 kip) at a displacement of 60.8 mm (2.4 in.).

Series II: Loading parallel to the axis of the masonry beam Under parallel forces, the loading direction also generated disparities in the capacity of side-bearing connections. The load capacity of the specimen tested under pushing (SB-CP-D) was 2.26 times that of its counterpart tested under a pulling force (SB-TP-D). While specimen SB-TP-D peaked at 7.8 kN (1.8 kip) under pulling at a displacement of 17.6 mm (0.7 in.), specimen SB-CP-D was able to reach a load of 17.0 kN (3.8 kip) but at a displacement of 82.5 mm (3.2 in.).

For this connection subjected to pushing and pulling forces, it would be expected that the peak failure loads and displacements would be similar; however, there was a large difference in both the peak load and corresponding displacements between SB-TP-D and SB-CP-D. This is most likely because the drilled hole in specimen SB-TP-D had a slightly larger diameter, which compromised the tight fit of the connection bar with the masonry beam. It is worth mentioning that the slightly large hole diameter was done to fit the bar into the shear key between the two hollow-core slabs. This implies that the dry-fit drilled connection was sensitive to the installation, with a snug fit being critical to the load resistance.

The disparity of capacity shown in Fig. 8 indicates that both end-bearing and side-bearing connections were more susceptible to failure under pulling forces than pushing forces, regardless of load orientation. It should be noted that none of the connection bars attained the nominal tensile yield capacity of 40 kN (9 kip), regardless of loading direction, load orientation, or bearing type.

Strains in the connection bar

Figure 9 illustrates the load-strain relationship of the connection bar in end- and side-bearing connections. Strains were measured at the top surface of the masonry beam. An additional strain gauge was placed at the grouted bend of the connection bar. Because the readings of this strain gauge were smaller than 450 $\mu\epsilon$ in all tested specimens, those results are not presented herein. The following section discusses the load-strain relationship for the connection bar at the interface between the hollow-core slab and the masonry beam.

Series I: Loading normal to the axis of the masonry beam Under compression, the connection bars in end-bearing specimens EB-CN-D and EB-CN-A showed an initial linear

elastic stage with compressive strains in the range of -100 to -300 $\mu\epsilon$, respectively, followed by reversed tensile strains. These tensile strains were caused by the slab pulling out the connection bar while being pushed. Then, both strain curves started to diverge and experienced a different peak for each connection, which was associated with the onset of concrete cover spalling. At this time, the longitudinal reinforcement in the masonry beam acted as dowels, interlocking the cracked faces of the masonry blocks and the grout. Consequently, the connection bars in both specimens were able to develop larger strains in the post-peak stage. For specimen EB-CN-D, at 80% of the peak load, the connection bar reached yielding while the beam showed considerable damage. At peak load, the measured tensile strains were 16,000 $\mu\epsilon$, which demonstrated great ductility before failure.

On the other hand, the connection bar with adhesive (EB-CN-A) reached the peak load of 29.0 kN (6.5 kip) at a strain of only 650 $\mu\epsilon$. Following a small load drop of 1.7 kN (0.4 kip) (5.9%), the bar yielded at a load of 27.3 kN (6.1 kip) and this load remained relatively steady until 3380 $\mu\epsilon$. The connection then experienced a slight decrease in strength associated with large strains up to 19,000 $\mu\epsilon$. After this point, the strain gauge malfunctioned, but a load reduction was observed while the masonry beam experienced more severe spalling until it crushed. Although this connection with adhesive (EB-CN-A) resisted larger loads, it offered less ductility than its counterpart without adhesive (EB-CN-D). This may be attributed to the stronger load transfer mechanism when an adhesive is used versus the dry-fit method because the masonry beam in specimen EB-CN-A survived a larger load and more damage than specimen EB-CN-D at bar yielding.

In contrast, the measured strains in the connection bars of end-bearing specimens tested under tension (pulling) forces, EB-TN-D and EB-TN-A, were considerably lower at the peak load. The first peak, triggered by the onset of cover spalling, occurred when the measured strains were 325 and 380 $\mu\epsilon$ in specimens EB-TN-D and EB-TN-A, respectively. Afterward, the load dropped and the curves diverged. The dry-fit connection bar (EB-TN-D) experienced concrete cover and grout spalling and bar pullout, leading to strength degradation without any further strain increase; the connection bar with adhesive (EB-TN-A) had a second peak where the measured strains reached 2110 $\mu\epsilon$. Even though the load did not significantly increase compared with the first peak, the use of adhesive delayed the failure and demonstrated more ductility.

Series I: Loading parallel to the axis of the masonry beam When subjected to parallel pushing forces, the bar in the end-bearing connection (EB-CP-D) exhibited a similar load-strain behavior to its counterpart tested under normal pushing (EB-CN-D). After the initial linear elastic stage, the connection bar yielded at 70% of the peak load (Fig. 9). The post-peak descending part of the graph resulted from bar pullout, where the bar continued accumulating strains while bending in the direction of the load. A second peak occurred at a load of 25.9 kN (5.8 kip), which is not shown on the

curve because the strain gauge malfunctioned after reading 10,870 $\mu\epsilon$ at a load of 17.1 kN (3.8 kip). However, this exhibited great ductility and ample warning before failure.

Series II: Loading normal to the axis of the masonry beam
beam The connection bar in the side-bearing connection test-

ed under compression (pushing) forces (SB-CN-D) initially developed compressive strains similar to its counterpart with the end-bearing type connection (Fig. 9). These compressive strains achieved up to -425 $\mu\epsilon$ and then shifted to tensile strains at a load of approximately 13.2 kN (3 kip). Afterward, the connection bar yielded at 85.8% of the peak load. A small

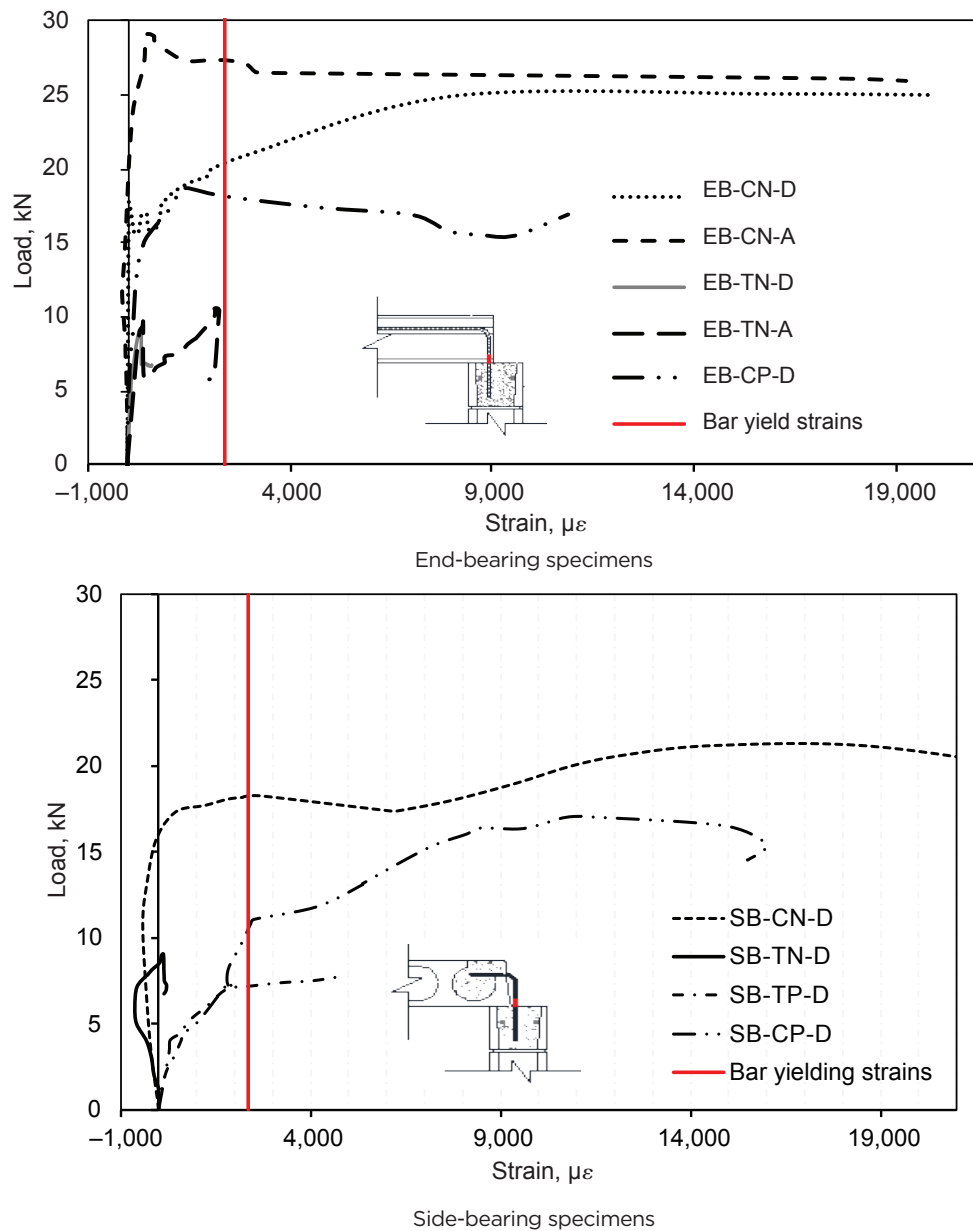


Figure 9. Load-strain relationships. Note: EB-CN-A = end-bearing specimen with compression load applied normal to the masonry beam and connection bars bonded with adhesive; EB-CN-D = end-bearing specimen with compression load applied normal to the masonry beam and dry-fit connection bars; EB-CP-D = end-bearing specimen with compression load applied parallel to the masonry beam and dry-fit connection bars; EB-TN-A = end-bearing specimen with tension load applied normal to the masonry beam and connection bars bonded with adhesive; EB-TN-D = end-bearing specimen with tension load applied normal to the masonry beam and dry-fit connection bars; SB-CN-D = side-bearing specimen with compression load applied normal to the masonry beam and dry-fit connection bars; SB-CP-D = side-bearing specimen with tension load applied parallel to the masonry beam and dry-fit connection bars; SB-TN-D = side-bearing specimen with tension load applied normal to the masonry beam and dry-fit connection bar; SB-TP-D = side-bearing specimen with tension load applied parallel to the masonry beam and dry-fit connection bars. 1 kN = 0.225 kip.

load drop followed because of initial concrete cover spalling and bar pullout. At the second peak, the strains in the connection bar were $18,650 \mu\epsilon$.

On the other hand, similar to its counterpart with the end-bearing type connection, under tension (pulling) forces it developed considerably smaller strains and lower capacity compared with SB-CN-D. The connection bar initially experienced compressive strains, resulting from an unintended slight bar inclination when it was inserted, which provoked the slabs to push the bar against the beam. These compressive strains reached $-620 \mu\epsilon$. Once the connection bar recovered the vertical position after further slab pulling, the bar experienced tensile strains. However, the connection bar developed only $110 \mu\epsilon$ when the hollow-core slabs had been pushed to their end of bearing. This may be attributed to the bar pullout.

In general, the test results show that the connection bar tested under normal pushing forces gave ample warning before attaining the maximum load capacity, regardless of bearing type. In contrast, when the connection bar was subjected to pulling normal forces, it developed considerably lower strains, resulting in a low lateral capacity and lack of ductility before failure.

Series II: Loading parallel to the axis of the masonry beam When subjected to parallel forces, the connection bars of side-bearing specimens SB-CP-D and SB-TP-D had a bilinear load-strain relationship under either pushing or pulling (Fig. 9). Both connection bars experienced tensile stresses due to bar pullout and bending in the direction of the force. After the initial linear elastic stage, the curves showed a slope reduction at bar yielding in both specimens. While the connection bar subjected to pushing (SB-CP-D) yielded at 63.5% of the peak load, the connection bar in the specimen under pulling (SB-TP-D) yielded at 92.3% of the peak load. The latter connection bar (SB-TP-D) experienced large deformation and bending but did not significantly increase the load-carrying capacity in the postyielding stage.

Although the connection bars reached yielding under pushing forces regardless of load orientation or bearing type, the yielding load was considerably smaller than the predicted direct tension value of 40 kN (9 kip), based on material properties (Table 2). Under pulling forces, the capacity of the connection bars was even lower, where the yielding load was either close to one-fourth of the predicted value or the bars did not yield. These relatively low yielding loads resulted from the eccentricity of the applied in-plane force with respect to the location of the connection bar (interface of the slabs with the masonry beam [Fig. 2]). This load eccentricity provoked the bar bending and early yielding.

Bar bending in the direction of the force was due to bar pullout in the case of dry-fit connections and due to grout spalling in the case of connections with adhesive, which left part of the bar exposed. Depending on other factors related to the connection detail, such as bar cover in grout and formation of initial cracks in the masonry beam, the onset of bar bending in the direction

of the force occurred earlier. When cracks appeared at the reinforcement location, the tight fit of the bar was compromised, leading to bar pullout, bending, and thereof yielding sooner than expected. Side-bearing connections were more vulnerable to this effect because a segment of the bar was not embedded in grout, causing relatively lower yielding loads.

Displacement of the slabs

Figure 10 presents the load-slab displacement relationship of bearing connections for series I and II. The curves repeatedly show bumps in their slopes in specimens with adhesive, which are associated with cycles of bar yielding and pullout as well as masonry beam cracking and load accommodation, which can cause small load drops in the ascending load-displacement relationship.

Series I: Loading normal to the axis of the masonry beam The load-displacement relationships of bearing connections under normal forces—EB-CN-A, EB-CN-D, EB-TN-A and EB-TN-D—initially exhibit linear elastic behavior with comparable slopes (Fig. 12). The graphs diverge at their first peak load. For the specimen under compression (pushing) forces with dry-fit bars (EB-CN-D), the first peak, caused by the development of additional cracks, was the beginning of bar pullout and yielding. This caused a slope reduction and provoked excessive slab displacement (84.4 mm [3.3 in.]) at peak load; however, its counterpart with adhesive (EB-CN-A) tested under compression forces attained a larger peak load of 29.0 kN (6.5 kip) at a displacement of 8.7 mm (0.3 in.) at the end of the linear elastic stage. This indicates a stiffer response when incorporating the adhesive to the connection. The post-peak stage in the latter specimen showed strength degradation, where the load decreased while the displacement increased rapidly. The changes in the slope became more negatively abrupt as the beam suffered more spalling, until finally beam crushing occurred.

Under tension (pulling) forces, end-bearing specimens EB-TN-D and EB-TN-A reached the first peak of 9.1 kN (2 kip) at a displacement of 3.5 mm (0.14 in.) and 9.9 kN (2.2 kip) at a displacement of 5.4 mm (0.2 in.), respectively. While the connection with dry-fit bar, EB-TN-D, suffered strength degradation after the peak load due to cover spalling, the connection with the adhesive, EB-TN-A, experienced a second peak of 10.6 kN (2.4 kip) at a displacement of 36.4 mm (1.4 in.); however, both specimens displayed low stiffness and allowed excessive slab displacements under low values of load.

Series I: Loading parallel to the axis of the masonry beam The connection bar in the end-bearing specimen, EB-CP-D, exhibited a load-slab displacement relationship similar to its counterpart under normal compression forces (Fig. 10). After the initial linear elastic stage, a slope reduction and series of bumps followed due to bar pullout and yielding. At peak load, the displacement of the slab was 112 mm (4.4 in.).

The excessively large displacement values at peak load in

end-bearing connection under compression and shear forces (EB-CN-D and EB-CP-D) reflect the lack of stiffness in connections with dry-fit bars resulting in bar pullout. Although there were no potential hazards related to bearing loss under compression forces, such a large displacement after the second crack might cause floor misalignments, bumping with adjacent units, and overall loss of integrity.

As indicated in the Canadian Standards,^{2,4} the slabs supported on masonry have a minimum seating length of 50 mm (2 in.) or $l_n/180$, whichever is greater, where l_n is the clear span between supports of the hollow-core slabs. During the construction of the test specimens, this value was exceeded to ensure a controlled failure; however, the slabs displaced considerably under tension forces in specimen EB-TN-D once the concrete cover was lost.

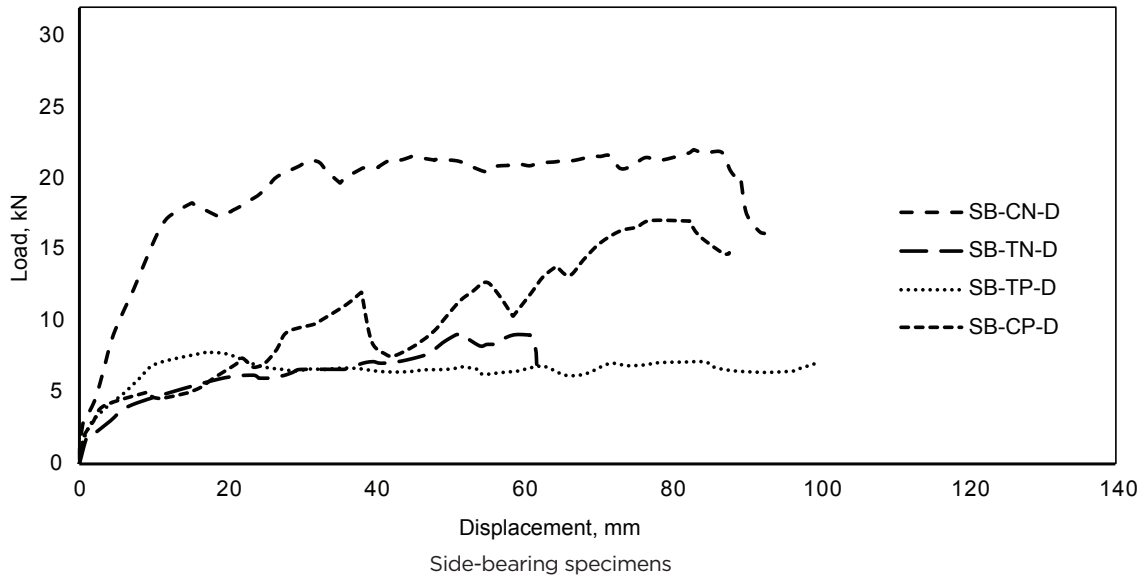
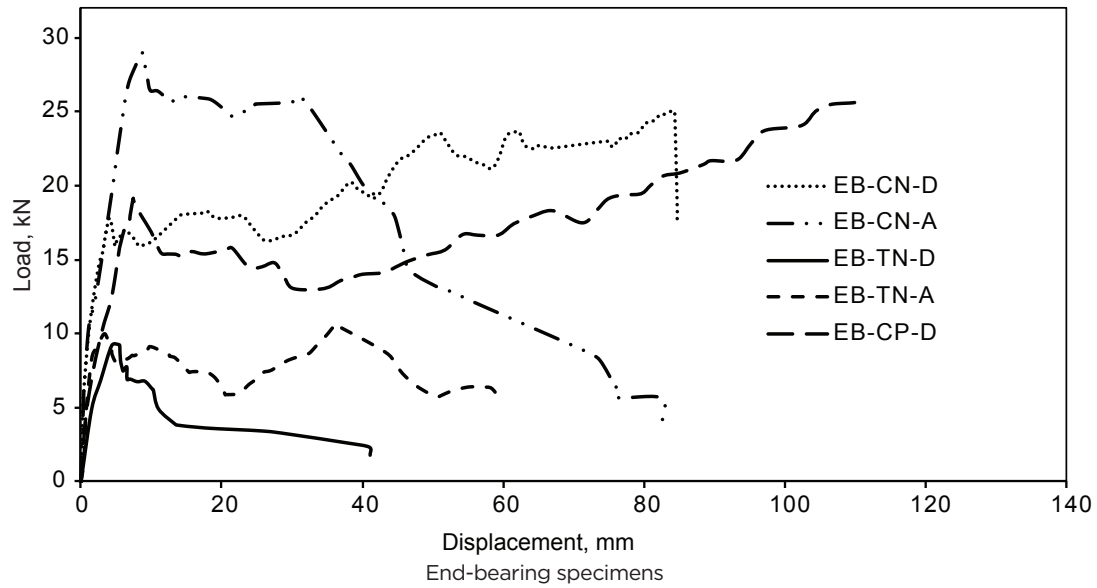


Figure 10. Load–displacement relationships. Note: EB-CN-A = end-bearing specimen with compression load applied normal to the masonry beam and connection bars bonded with adhesive; EB-CN-D = end-bearing specimen with compression load applied normal to the masonry beam and dry-fit connection bars; EB-CP-D = end-bearing specimen with compression load applied parallel to the masonry beam and dry-fit connection bars; EB-TN-A = end-bearing specimen with tension load applied normal to the masonry beam and connection bars bonded with adhesive; EB-TN-D = end-bearing specimen with tension load applied normal to the masonry beam and dry-fit connection bars; SB-CN-D = side-bearing specimen with compression load applied normal to the masonry beam and dry-fit connection bars; SB-CP-D = side-bearing specimen with compression load applied parallel to the masonry beam and dry-fit connection bars; SB-TN-D = side-bearing specimen with tension load applied normal to the masonry beam and dry-fit connection bar; SB-TP-D = side-bearing specimen with tension load applied parallel to the masonry beam and dry-fit connection bars. 1 mm = 0.0394 in.; 1 kN = 0.225 kip.

This could result in loss of bearing of the slabs under relatively low loads. In the test specimens incorporating an adhesive mitigated the lack of stiffness and delayed the loss of bearing but did not allow the load to be increased to the acceptable values for integrity ties in buildings of three or more stories.

Series II: Loading normal to the axis of the masonry beam

The load-displacement curves for side-bearing specimens exhibited significantly lower slopes compared with their end-bearing counterparts (Fig. 10). The stiffness disparities were caused by variations in the connection details between end-bearing and side-bearing connections. The bars in the end-bearing specimens were enclosed between the two slabs and fully embedded in the grout, while the bars in the side-bearing specimens were partially unrestrained and external to the slab. The latter configuration significantly reduced the stiffness of the side-bearing connections.

Out of the four graphs in Fig. 10, the curve for the side-bearing connection tested under compression normal forces (SB-CN-D) presents the steepest slope. This resulted from the bar leaning against the hollow-core slab under the pushing loads. Following the initial linear elastic stage, the connection suffered bar pullout, bar yielding, and slope reduction. In this specimen, the measured slab displacement was 83.1 mm (3.3 in.) when beam crushing occurred at the peak load. In contrast, under tension (pulling) forces, the connection bar in specimen SB-TN-D was completely unrestrained, which provoked the bar pullout and compromised the load transfer to the supporting beam, evidenced by few cracks and no spalling observed before the loss of bearing. The test was stopped when the displacement reached 60.8 mm (2.4 in.).

Series II: Loading parallel to the axis of the masonry beam

Although the side-bearing connection under pushing force (SB-CP-D) had a steeper load-displacement curve compared with the specimen under pulling forces (SB-TP-D), both connections allowed excessive displacements and bar pullout (Fig. 10) and displayed low stiffness. The testing of specimens SB-CP-D and SB-TP-D was stopped once the slabs displaced 100 and 88 mm (3.9 and 3.5 in.), respectively, and no further load increase occurred. The test was halted to ensure the slabs did not lose bearing on the masonry beam, which might result in a safety hazard.

In general, slab SB-TP-D tested under parallel shear forces can be considered the most critical load-case scenario with the most undesirable mode of failure because the connection bar had the lowest peak and yielding loads and the bar continued to pull out easily, leading to the largest slab displacement measured. As previously noted, the drilled hole for the bar dowel in slab SB-TP-D was not as snug to the bar as for slab SB-CP-D, which is the likely explanation for the much lower peak load.

Conclusion

Based on the analysis of the test results, the following conclusions can be drawn:

- The loading direction significantly influenced the mode of failure of dry-fit connection bars under loads normal to masonry supports, regardless of bearing type. Under compression forces, the reinforcing bar connections failed by grout crushing preceded by bar pullout and yielding. Under tension forces, the connections failed by bar pullout and loss of bearing.
- The mode of failure of connections tested under parallel shear forces was governed by bar pullout and yielding, regardless of load direction and type of bearing.
- The longitudinal reinforcement of the masonry beam significantly contributed to the ductile behavior of the connection. This reinforcement acted as dowels after the development of cracks in the masonry beam and maintained the integrity of the masonry block.
- The behavior of the end-bearing connections differed from that of the side-bearing connections under parallel loading and normal pulling. The unrestrained bar in side-bearing connections displayed lower stiffness under tension (pulling) and shear forces than its end-bearing counterpart. In addition, the side-bearing connections attained lower capacity than their end-bearing counterparts, regardless of load orientation and direction.
- The connection bar with adhesive displayed more capacity, stronger fixation, and better load transfer to the supporting beam compared with the connections with dry-fit bars.
- The tested capacity of the end-bearing connections under tension (pulling) forces met the North American code requirements for resisting minimum structural integrity forces for a building of up to two stories but did not satisfy the specifications for buildings of three or more stories.^{2,3}
- The tested tensile capacities of the end-bearing connections represent lower-bound, conservative values because no gravity loads were added. The clamping effect of gravity loads on the end-bearing connection from long-span hollow-core slabs coupled with the weight of upper-story walls would likely delay the large lateral displacements observed during testing and result in larger load capacities. In addition, the increased compressive strength of cast-in-place or precast concrete walls compared with masonry block wall and grout strength would also increase the load capacity of the connection, at which the dowels would crack the wall surface under tension loading.
- The configuration of the L-shaped connection detail used in this study generated load eccentricities when in-plane forces act on hollow-core slab floors. As a result, bending of the connection bar occurred at early stages, which were triggered by cracking, cover spalling, and bar pullout. This bar bending resulted in bar yielding at relatively low levels of load, causing low capacities.

- Reducing the connection load path eccentricity by aligning the connection bar with the horizontal plane of the hollow-core slabs put the bar into more direct tension, resulting in a higher lateral capacity and a lower lateral displacement. This can be achieved by hooking connection bars into of the boundary reinforcement of the hollow-core slab diaphragm or by tying hooked connection bars directly behind the vertical dowels. Ideally the connection between the hollow-core slabs and the masonry wall should be detailed such that the connection bar will be able to develop the full yield capacity of the connection bars in tension for ductility under potential overloading scenarios and would also meet the design intent of the North American design codes (CSA A23.3-19² and ACI 318-19³) for structural integrity reinforcement.
- Future testing with the connection bar in-plane with the hollow-core slab grout keys should be investigated, including a portion of the wall extending above and below the level of the hollow-core slabs to reflect the load response of an intermediate level bearing wall accurately for tension end-bearing connections. Tests could be performed with and without a clamping force in the wall at the connection, to confirm the effect of gravity loads on the connection response for capacity, displacement, and failure mode.

Acknowledgments

The authors would like to express their gratitude for the financial support provided by the Canadian Precast/Prestressed Concrete Institute and the Natural Sciences and Engineering Research Council of Canada. Furthermore, the in-kind contributions received from Armtex Precast (Infrastructure Solutions), Tower Engineering Group, and Manitoba Masonry Institute are gratefully acknowledged. Special thanks also goes to the technical staff of the W. R. McQuade Structures Laboratory at the University of Manitoba for their assistance during the experimental work.

References

1. Brian J. Hall, managing director at Canadian Precast/Prestressed Concrete Institute, email message to author, April 12, 2021.
2. CSA Group. 2019. *Design of Concrete Structures*. CSA A23.3-19. Toronto, ON, Canada: CSA Group.
3. ACI (American Concrete Institute) Committee 318. 2019. *Building Code Requirements for Structural Concrete (ACI 318-19) and Commentary (ACI 318R-19)*. Farmington Hills, MI: ACI.
4. CPCI (Canadian Precast/Prestressed Concrete Institute). 2017. *CPCI Design Manual: Precast and Prestressed Concrete*. Ottawa, ON, Canada: CPCI.
5. PCI Hollow Core Slab Producers Committee. 2015. *PCI Manual for the Design of Hollow Core Slabs and Walls*. MNL-126. 3rd ed. Chicago, IL: PCI. <https://doi.org/10.15554/MNL-126-15>.
6. Herlihy, M. D. 1999. "Precast Concrete Floor Support and Diaphragm Action." PhD diss., Department of Civil Engineering, University of Canterbury, Christchurch, New Zealand.
7. Lindsay, R. A., J. B. Mander, and D. K. Bull. 2004. "Experiments on the Seismic Performance of Hollow-Core Floor Systems in Precast Concrete Buildings." In *13th World Conference on Earthquake Engineering Proceedings, August 1–6, 2004, Vancouver, BC, Canada*. Vancouver, BC: 13 WCEE Secretariat.
8. MacPherson, C. J., J. B. Mander, and D. K. Bull. 2005. "Reinforced Concrete Seating Details of Hollow-Core Floor Systems." In *2005 NZSEE Conference Proceedings, March 11–13, 2005, Taupo, New Zealand*. Wellington, New Zealand: New Zealand Society for Earthquake Engineering. <http://db.nzsee.org.nz/2005/Paper24.pdf>.
9. Matthews, J. 2004. "Hollow-core Floor Slab Performance Following a Severe Earthquake." PhD diss., Department of Civil Engineering, University of Canterbury, Christchurch, New Zealand.
10. Mejia-McMaster, J. C., and R. Park, R. 1994. "Tests on Special Reinforcement for the End Support of Hollow-Core Slabs." *PCI Journal* 39 (5): 90–105. <https://doi.org/10.15554/pcij.09011994.90.105>.
11. ASTM International. 2021. *Standard Test Methods and Definitions for Mechanical Testing of Steel Products*. ASTM A370-20. West Conshohocken, PA: ASTM International. <https://doi.org/10.1520/A0370-21>.
12. ASTM International. 2021. *Standard Test Method for Compressive Strength of Hydraulic Cement Mortars (Using 2-in. or [50 mm] Cube Specimens)*. ASTM C109/C109M. West Conshohocken, PA: ASTM International. https://doi.org/10.1520/C0109_C0109M-21.

Notation

l_n = clear span between supports of the hollow-core slab

About the authors



Susana Hernandez Brito is a master of science student in the Department of Civil Engineering at the University of Manitoba in Winnipeg, MB, Canada.



Karam Mahmoud, PhD, PEng, is a structural engineer at Tetra Tech in Winnipeg and a former postdoctoral fellow in the Department of Civil Engineering at the University of Manitoba.



Karl Truderung, MSc, PEng, is a structural engineer and associate at Tower Engineering Group in Winnipeg.



Ehab El-Salakawy, PhD, PEng, is a professor in the Department of Civil Engineering at the University of Manitoba and was the Canada Research Chair in Durability and Modernization of Civil Structures from 2006 to 2016.

Abstract

Integrity ties are necessary in hollow-core slab floors as connections to prevent floor displacements under lateral loads and maintain the overall structural integrity of buildings. In Eastern Canada, the integrity tie for hollow-core slabs on masonry walls usually consists of a 10M (no. 3), L-shaped steel bar that is hammered into the supporting wall and grouted to the slabs. However, current North American design codes do not offer sufficient provisions to determine the capacity or predict the mode of failure of these ties and connections. This paper introduces the results of testing nine full-scale reinforcing bar connection assemblies under monotonic in-plane forces (compression, tension, and shear) until failure. Test parameters in this study included direction and orientation of the in-plane loading, the bearing type of the hollow-core slabs, and the use of adhesive.

Test results showed that connections with dry-fit bars tested under compression failed by bar yielding followed by masonry beam crushing. In addition, the mode of failure under tension forces was governed by the loss of bearing of the slabs due to bar pullout and cover spalling. Under shear forces, the connection failed by bar yielding. Finally, the connections with adhesive had a similar mode of failure compared to their counterparts with dry-fit bars, but these did not show bar pullout from the masonry beam, therefore demonstrating higher stiffness.

Keywords

Beam, connection, end-bearing connection, force, hollow-core, in-plane force, integrity tie, lateral load, masonry, side-bearing connection, slab, tension.

Review policy

This paper was reviewed in accordance with the Precast/Prestressed Concrete Institute's peer-review process. The Precast/Prestressed Concrete Institute is not responsible for statements made by authors of papers in *PCI Journal*. No payment is offered.

Publishing details

This paper appears in *PCI Journal* (ISSN 0887-9672) V. 67, No. 6, November–December 2022 and can be found at <https://doi.org/10.15554/pcij67.6-03>. *PCI Journal* is published bimonthly by the Precast/Prestressed Concrete Institute, 8770 W. Bryn Mawr Ave., Suite 1150, Chicago, IL 60631. Copyright © 2022, Precast/Prestressed Concrete Institute.

Reader comments

Please address any reader comments to *PCI Journal* editor-in-chief Tom Klemens at tklemens@pci.org or Precast/Prestressed Concrete Institute, c/o *PCI Journal*, 8770 W. Bryn Mawr Ave., Suite 1150, Chicago, IL 60631. [f](#)